ARTICLE

Synthesis of Strongly Fluorescent Graphene Quantum Dots by Cage-Opening Buckminsterfullerene

Chun Kiang Chua,[†] Zdeněk Sofer,[‡] Petr Šimek,[‡] Ondřej Jankovský,[‡] Kateřina Klímová,[‡] Snejana Bakardjieva,[§] Štěpánka Hrdličková Kučková,[∥] and Martin Pumera*[,†]

[†]Division of Chemistry & Biological Chemistry, School of Physical and Mathematical Sciences, Nanyang Technological University, Singapore 637371, Singapore, [‡]Department of Inorganic Chemistry, University of Chemistry and Technology Prague, Technická 5, 166 28 Prague 6, Czech Republic, [§]Centre of Instrumental Techniques, Institute of Inorganic Chemistry of the AS CR, v.v.i., Husinec-Rez c.p. 1001, 250 68 Rez, Czech Republic, and [∥]Department of Biochemistry and Microbiology, University of Chemistry and Technology Prague, Technická 5, 166 28 Prague 6, Czech Republic

ABSTRACT Graphene quantum dots is a class of graphene nanomaterials with exceptional luminescence properties. Precise dimension control of graphene quantum dots produced by chemical synthesis methods is currently difficult to achieve and usually provides a range of sizes from 3 to 25 nm. In this work, fullerene C_{60} is used as starting material, due to its well-defined dimension, to produce very small graphene quantum dots (~2−3 nm). Treatment of fullerene C_{60} with a mixture of strong acid and chemical oxidant induced the oxidation, cage-opening, and fragmentation processes of fullerene C_{60}. The synthesized quantum dots were characterized and supported by LDI-TOF MS, TEM, XRD, XPS, AFM, STM, FTIR, DLS, Raman spectroscopy, and luminescence analyses. The quantum dots remained fully dispersed in aqueous suspension and exhibited strong luminescence properties, with the highest intensity at 460 nm under a 340 nm excitation wavelength. Further chemical treatments with hydrazine hydrate and hydroxylamine resulted in red- and blue-shift of the luminescence, respectively.

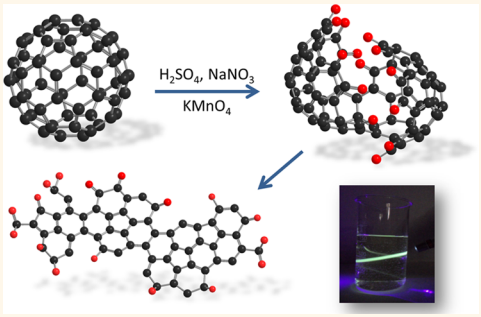

KEYWORDS: quantum dots · luminescence · fullerenes · graphene · oxidation

The properties of graphene are closely governed by its geometry and chemical compositions. Such size-dependent properties can be observed in graphene nanoribbons and graphene nanoplatelets.[1,2] Graphene quantum dots (graphene QDs) represent a class of zero-dimensional carbon nanoparticles with typical dimensions of *ca.* <20 nm.[3,4] The low dimension of graphene QDs leads to unique quantum confinement[5] and edge effects resulting in exceptional fluorescence properties.[6,7] Due to the high surface area, potential biocompatibility or low toxicity, and the availability of a $\pi-\pi$ conjugated network with functionalizable surface groups, graphene QDs have been envisioned to fuel the development of research in electrochemical biosensors, drug delivery, bioimaging, and energy conversion.[6,8]

Akin to the synthesis of graphene, graphene QDs can be prepared by either a top-down or bottom-up approach. The top-down approach involves cutting graphene sheets into graphene QDs by chemical ablation,[9−13] mechanical grinding,[14] or electrochemical synthesis.[15] On top of the requirement for expensive equipment, such treatments are usually difficult to control and often provide graphene QDs of various diameters (3−25 nm). Apart from that, the bottom-up approach includes chemical synthesis[16,17] and ruthenium-catalyzed cage-opening of fullerene C_{60}.[18] Although the synthesis of graphene QDs with specific sizes can be anticipated, the former involves tedious synthetic procedures, while the latter requires sophisticated equipment. With the current challenges and limitations, it is thus worthwhile to develop more efficient and affordable alternatives that are able to produce high-quality graphene QDs of specific sizes. Besides that, the fabrication of well-defined tiny graphene QDs (~2−3 nm) will be advantageous for numerous applications. For example, the low toxicity of

* Address correspondence to pumera.research@gmail.com.

Received for review October 3, 2014 and accepted March 4, 2015.

Published online March 11, 2015
10.1021/nn505639q

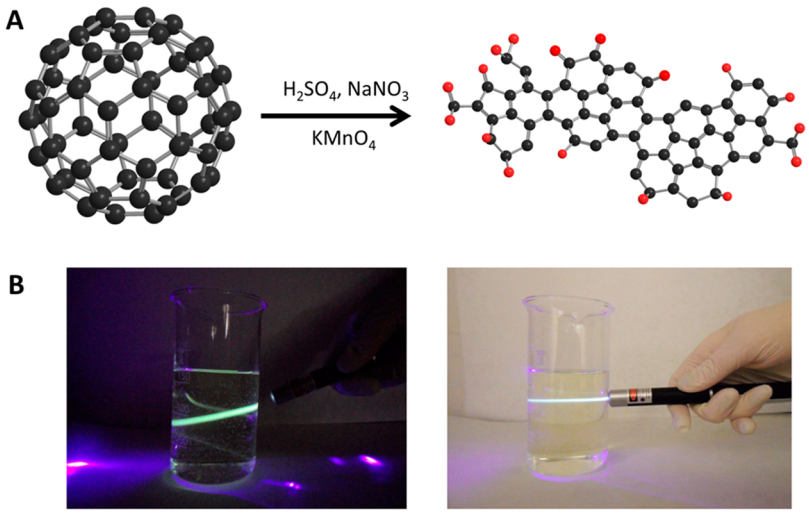

Figure 1. (A) Illustration of the oxidation and cage-opening of fullerene C_{60} with treatment of strong acid and chemical oxidant. (B) Luminescence of graphene QDs excited with a blue laser pointer (405 nm).

graphene QDs as compared to standard fluorescence probes using $A^{II}B^{VI}$ semiconductors like CdSe or rare earth fluorides rendered it valuable.

In fact, this has motivated us to investigate the possibility of cage-opening fullerene C_{60}, which is a well-defined carbon nanomaterial with a diameter of ~1 nm, *via* a top-down wet chemistry approach. As a spherical molecule, fullerene C_{60}, or buckminsterfullerene, is made up of 60 carbon atoms packed into fused hexagons and pentagons.[19] As the main chemical reactivity principle of fullerene C_{60} is based on relieving the strain of the fullerene C_{60} cage, various derivatization reactions including cycloaddition, free radical addition, nucleophilic addition, and halogenation have been achieved.[20] In conjunction, the unzipping of carbon nanotubes to produce graphene nanoribbons under the presence of strong acid and oxidant has inspired us to investigate the possible cage-opening of fullerene C_{60} based on similar chemical treatment. As such, the treatment of fullerene C_{60} with concentrated sulfuric acid and potassium permanganate oxidant based on the modified Hummers method is anticipated to yield graphene quantum dots with well-defined diameters of 2−3 nm. The obtained graphene QDs were characterized by laser desorption ionization with time-of-flight mass spectrometry (LDI-TOF MS), transmission electron microscopy (TEM), X-ray diffraction (XRD), atomic force microscopy (AFM), scanning tunneling microscopy (STM), Raman spectroscopy, Fourier transform infrared (FT-IR), X-ray photoelectron spectroscopy (XPS), dynamic light scattering (DLS), and luminescence analyses.

Further confirmation of the generation of graphene QDs, which should be highly oxidized due to the usage of concentrated acid and strong oxidant, was achieved by subsequent extensive chemical modifications. This includes esterification with trifluoroacetic anhydride and 4-nitrobenzoyl chloride, reduction with hydrazine hydrate, and reactions with hydroxylamine. In fact, the chemical modifications were accompanied by obvious changes on the luminescence properties of the modified graphene QDs.

RESULTS AND DISCUSSION

The cage-opening of fullerene C_{60} was attempted by subjecting it to a mixture of concentrated sulfuric acid, sodium nitrate, and potassium permanganate according to the modified Hummers method.[21] Similar chemical treatment has been performed to yield carbon nanoribbons from carbon nanotubes.[22] The reaction scheme is shown in Figure 1A. It was observed in the case of fullerene C_{60} that the quenched reaction mixture was clear yellow with negligible precipitation. In order to remove any soluble reaction byproducts, the clear yellow solution was dialyzed using a membrane with a cutoff below 1 kDa. The dialyzed material exhibited strong luminescence, as clearly visible in Figure 1B, where a blue laser pointer (405 nm) was used for luminescence excitation.

The successful oxidation/cage-opening of fullerene C_{60} was first investigated by LDI-TOF MS. This is a very sensitive method to detect highly stable fullerene clusters. The LDI-TOF MS spectra of fullerene C_{60} before and after the oxidation/cage-opening procedure are shown in Figure SI1 (Supporting Information) for comparison. Although the disappearance of the fullerene C_{60} peak upon oxidation/cage-opening was anticipated, it was by no means a definite indicator of the exact structure of the graphene QDs. Indeed as shown in Figure SI1A (Supporting Information), the presence of an intense peak at m/z = 720 confirmed the presence of fullerene C_{60}. Smaller carbon clusters were detected as well. The origin of small carbon clusters such as C_6^+, C_7^+, and C_8^+ has been reported not only for fullerenes[23] but also for graphite oxide that has

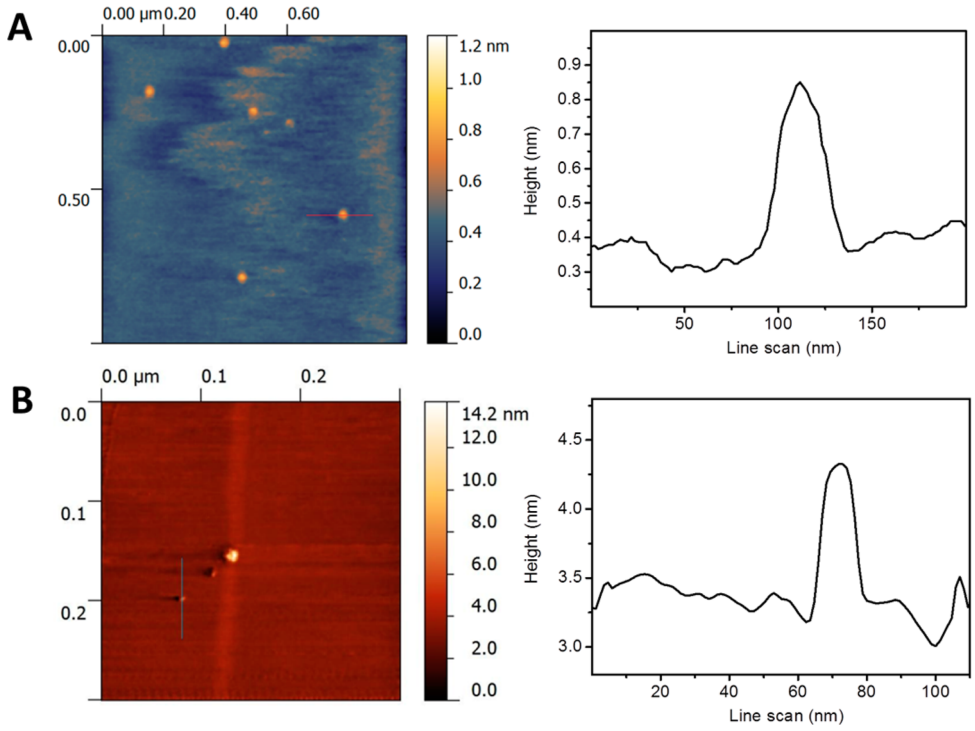

Figure 2. (A) AFM image of graphene QDs and the corresponding height profile for the indicated particle. (B) STM image of graphene QDs and the corresponding height profile for the indicated particle.

undergone thermal reduction.[24] The disappearance of the peak at m/z = 720 in the LDI-TOF MS spectrum of graphene QDs in Figure SI1B (Supporting Information) confirmed the successful oxidation/cage-opening of fullerene C_{60} into graphene QDs. Moreover, the absence of obvious peaks beyond m/z = 720 ruled out the presence of fullerenols and suggested possible fragmentation processes of the cage-opened C_{60}. In fact, only peaks of low m/z corresponding to small clusters that were composed of carbon, oxygen, and hydrogen were present.

The morphology of graphene QDs was further investigated using AFM and STM. The aggregation of graphene QDs during solvent evaporation was observed by AFM analysis in Figure 2A. Such aggregation originated from the formation of noncovalent interactions or weak hydrogen bonding between oxygen functional groups present on the graphene QDs' surface. The height of graphene QDs was about 0.6−1 nm and corresponded to typical values reported for graphene oxide and graphene nanoribbons.[1,25] Subsequent analysis with STM performed under constant-current mode showed graphene QDs with lateral sizes within the range 7−10 nm and a height of approximately 0.7 nm, as shown in Figure 2B. This corresponded to the DLS measurement, whereby particles of sizes up to 15 nm were observed. In fact, the particle size measured by DLS in Figure SI2 (Supporting Information) showed a hydrodynamic radius in the range 1−15 nm with a maximum at 3 nm, which coincided with the estimated lateral size of graphene QDs upon successful oxidation/cage-opening of C_{60}. The aggregation of graphene QDs in solution cannot be excluded since noncovalent interactions and hydrogen bonding between the oxygen functionalities are likely to occur. It should also be noted that the platelet characters of graphene QDs should be taken into account, and the relatively broad distribution indicated various orientations of platelet particles toward the laser and detector used for the measurements.

High-resolution TEM images were also collected to resolve the structure of the graphene QDs obtained from the oxidation/cage-opening of fullerene C_{60} (Figure SI3, Supporting Information). During the solvent evaporation process of the graphene QD suspension, aggregates were formed as also observed from AFM and STM analyses. Figure SI3A (Supporting Information) shows a low-magnification image of the graphene QD aggregates, while the electron diffraction pattern on the yellow-colored rectangular area in the inset confirmed the amorphous character of the graphene QD aggregates. A high-resolution image of the same aggregate shown in Figure SI3B (Supporting Information) supported the fully packed fullerene structure (fully packed graphene QDs were formed during the process of solvent evaporation). Subsequent high-resolution imaging in Figure SI3C (Supporting Information), which corresponded to the peripheral region of the aggregate (within the yellow oblong) in Figure SI3B (Supporting Information), showed the network geometry of graphene QDs in two adjacent blocks.

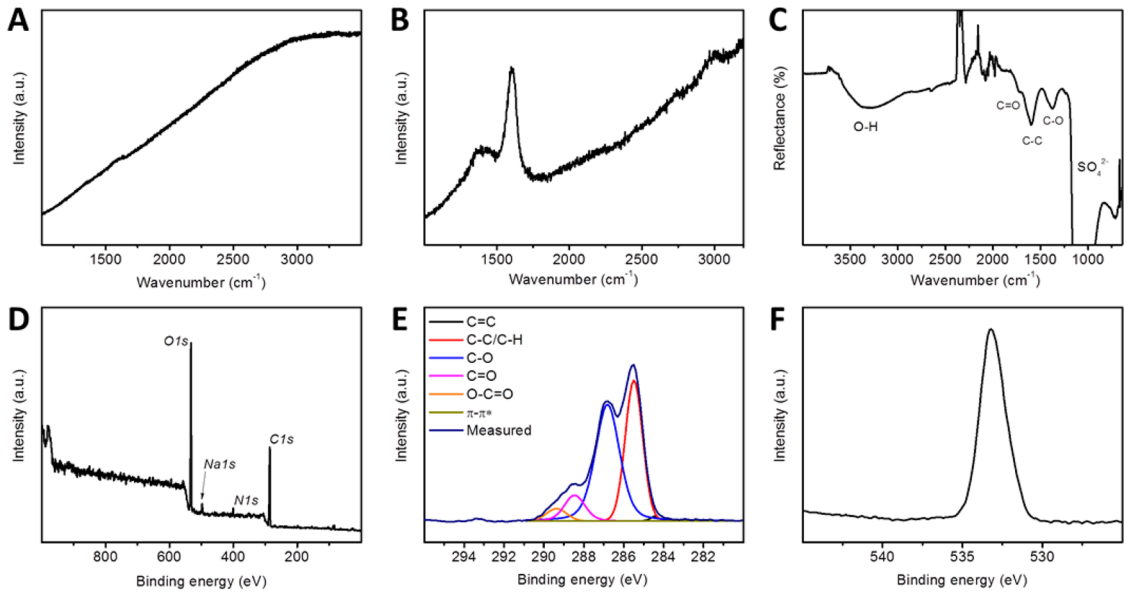

Figure 3. Raman spectra of graphene QDs measured with a (A) 532 nm laser at 5 W and (B) 325 nm laser at 2 mW. (C) FT-IR spectrum of graphene QDs obtained from the cage-opening of fullerene C_{60}. (D) Survey, high-resolution (E) C 1s and (F) O 1s core-level XPS spectra of graphene QDs. High-resolution N 1s core-level spectrum is provided in Figure SI4C in the Supporting Information.

Raman spectroscopy was subsequently performed to investigate the structure of graphene QDs. Two characteristic bands were observed on the graphene-based materials, mainly the D-band at 1350 cm^{-1} and G-band at 1580 cm^{-1}. The D-band is associated with sp^3-hybridized carbon atoms originating from defects and oxygen functional groups covalently bonded to the graphenic structure. The G-band arises from sp^2-hybridized carbon atoms. The computed intensity of D-band to G-band (D/G ratio) reflects the crystalline quality of the graphene-based material. It should be noted that the majority of Raman signals for materials exhibiting strong luminescence properties are often masked by the intense luminescence background. The Raman spectrum of graphene QDs measured with a 532 nm laser is shown in Figure 3A (Raman spectrum of fullerene C_{60} is shown in Figure SI4A, Supporting Information). The strong luminescence background formed by this excitation wavelength revealed only a weak G-band signal originating from sp^2-hybridized carbon atoms. To improve the signal-to-background ratio, a UV laser was subsequently used for the Raman measurement. The Raman spectrum of graphene QDs measured with a 325 nm laser is shown in Figure 3B. The strong G-band relative to the broad and low-intensity D-band indicated low disorder in the graphene QDs. The D/G ratio of graphene QDs was 0.41. This was drastically lower than typical values of D/G ratio observed on graphene oxide prepared from graphite. To note, contrasting Raman spectra obtained from lasers in the UV and vis regions have been reported by several authors on various carbon nanomaterials such as nanodiamonds and carbon nanotubes.[26−28] UV Raman spectroscopy typically exhibits a higher sensitivity toward carbon atoms with sp^3 hybridization (D-band), whereas excitation in the visible region leads to enhancement of signals originating from sp^2-hybridized carbon atoms (G-band). Due to this reason, the actual D/G ratio of graphene QDs can be even lower.

FT-IR spectroscopy enables the investigation of oxygen functional groups formed by the oxidation/cage-opening process of fullerene C_{60}. The FT-IR spectrum in Figure 3C clearly shows O−H stretching located around 3400 cm^{-1}. The peak at 1720 cm^{-1} due to C═O stretching proved the presence of a carboxylic acid group. Moreover, a C═O vibrational band was observed at 1370 cm^{-1}, whereas a weak shoulder at 1390 cm^{-1} was attributed to the C−O vibration of a carboxylic acid group. The C═C vibration of sp^2-hybridized carbon atoms was detected at 1600 cm^{-1}, while a strong band with a maximum at 1050 cm^{-1} was designated as C−O stretching. It was surprising to note that C−O stretching of the hydroxyl group resulted only in a very weak vibrational band at 1230 cm^{-1}. As a matter of fact, the presence of hydroxyl, ketone, and carboxylic acid functional groups indicated the successful cage-opening and a high degree of oxidation of fullerene C_{60}.

XPS analysis was consequently carried out to determine the chemical composition of graphene QDs. The XPS survey spectrum of graphene QDs presented in Figure 3D clearly shows C 1s and O 1s peaks at ~284.5 and ~533 eV, respectively. Na 1s and N 1s peaks were also detected at ~198 and ~400.5 eV, respectively. Further quantitative analysis indicated a distribution of 63.96 at. % of C, 30.87 at. % of O, 3.19 at. % of N, and 1.98 at. % of Na. A trace amount of nitrogen observed in

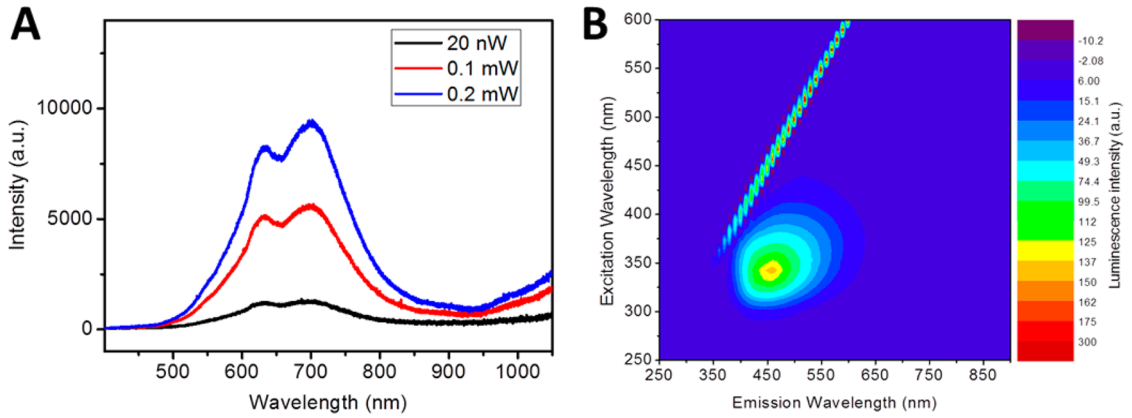

Figure 4. (A) Luminescence of graphene QDs in dry form obtained by excitation with a 325 nm laser using various laser powers of 20 nW, 0.1 mW, and 0.2 mW. Measurement was performed using a microphotoluminescence spectrometer (see Experimental Section). (B) Dependence of graphene QD luminescence on the wavelength of excitation light. High-intensity line originated from the scattering of excitation light. The measurement was performed on dialyzed graphene QDs on a Cary Eclipse (see Experimental Section).

graphene QDs was introduced during the oxidation/cage-opening procedure from the usage of $NaNO_3$ in conjunction with $KMnO_4$ as an oxidation agent.[29] Moreover, residues of sodium also originated from $NaNO_3$ as well as from NaOH, which was added to neutralize sulfuric acid prior to the dialysis purification process of graphene QDs. In fact, the relatively high content of oxygen confirmed the successful oxidation/cage-opening of fullerene C_{60}. The survey spectrum of fullerene C_{60} (Figure SI4B, Supporting Information) contained only a C 1s peak at ~285 eV without any traces of oxygen. Subsequently, a high-resolution C 1s core-level spectrum of graphene QDs was obtained. The C 1s peak in Figure 3E was fitted with Guassian–Lorentzian curves to quantitatively differentiate six different carbon moieties: C═C (284.4 eV), C–C/C–H (285.4 eV), C–O (286.3 eV), C═O (288.0 eV), O–C═O (289.0 eV), and a π–π* interaction (290.5 eV). The positions of the peaks were fitted according to typical fittings for graphite oxide.[30] The calculated abundances for the carbon functional groups were 0.8% C═C, 37.4% C–C/C–H, 48.9% C–O, 9.0% C═O, 3.8% O–C═O, and 0.1% π–π* interactions. In addition, a high-resolution O 1s core-level spectrum is shown in Figure 3F. The shape and binding energy peak position supported the C 1s core-level fitting results, whereby the majority of oxygen was bonded to carbon in the form of C–O. This was also in a good agreement with the data obtained from FT-IR spectroscopy that showed strong bands originating from the vibrations of the hydroxyl functional group.

Apart from that, the luminescence properties of graphene QDs were investigated using a tunable xenon light source and a microphotoluminescence system equipped with a He–Cd laser as excitation source. The almost linear dependence of luminescence intensity was observed for the excitation energy in the range from 20 nW to 0.2 mW. The obtained spectra are shown in Figure 4A. Broad luminescence was observed in the yellow-red region of the spectra with two maxima located at 630 and 700 nm. Especially for the application of quantum dots, it is very important to determine the luminescence intensity over the excitation wavelength. As such, graphene QDs were analyzed by a fluorimeter with a tunable excitation source using a Xe lamp on an aqueous suspension of the graphene QDs (Figure 4B). The highest intensity of luminescence was observed for 340 nm excitation wavelength with a maximum intensity at 460 nm. Obvious differences observed from the measurements on dry form and an aqueous suspension of graphene QDs indicated that the protonation of the carboxylic acid group as well as the interaction of other oxygen functional groups with water may critically affect the luminescence properties. Such drastic influences can originate from the very small size of the graphene QDs, which was formed only by several tenths of aromatic rings with a high concentration of oxygen functional groups, as determined by previous characterizations using various spectroscopic techniques. In fact, the synthesis of graphene QDs, which was performed several times to ascertain the reproducibility of the method, consistently gave graphene QDs with luminescence maxima in the range 450–465 nm (Figure SI5, Supporting Information).

Further chemical treatments on graphene QDs were performed to ascertain the presence and types of oxygen-containing groups. As summarized in Figure 5A, graphene QDs were subjected to treatment with trifluoroacetic anhydride, 4-nitrobenzoyl chloride, hydrazine hydrate, and hydroxylamine to target specific oxygen functionalities. The chemical modifications of graphene QDs were mainly determined by XPS analyses (Figures SI6–9, Supporting Information). The presence of hydroxyl groups on graphene QDs was verified by esterification reactions with trifluoroacetic

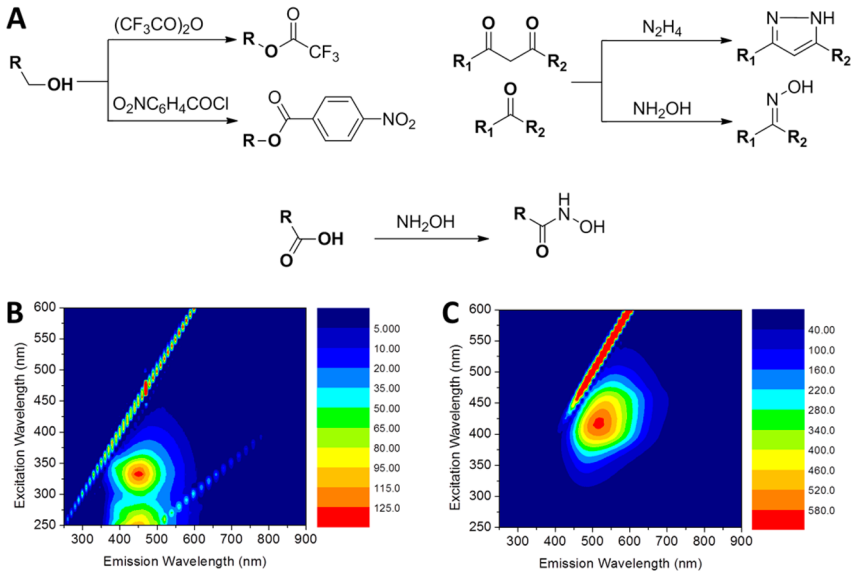

Figure 5. (A) Chemical transformation of functional groups on graphene QDs upon reactions with trifluoroacetic anhydride, 4-nitrobenzoyl chloride, hydrazine hydrate, and hydroxylamine. Dependence of graphene QD luminescence on the wavelength of excitation light for graphene QDs treated with (B) hydroxylamine and (C) hydrazine hydrate. High intensity of line originated from the scattering of excitation light.

anhydride (TFA) and 4-nitrobenzoyl chloride (NBC). The reactions were performed in dry phase whereby graphene QDs were suspended on a gold surface and treated with vapors of the reactants. XPS analyses on TFA-functionalized graphene QDs showed up to 2.9 at. % of fluorine (F/C ratio of 0.07). On the other hand, the reactivity of NBC with graphene QDs was lower than TFA given the moderate content of nitrogen (N/C ratio of 0.05). Nevertheless, the presence of a peak at 406 eV corresponding to the presence of a nitrophenyl group in the N 1s core-level spectrum of NBC-functionalized graphene QDs suggested the success of the functionalization. This characteristic peak was however not present on graphene QDs.

Graphene QDs were subsequently reacted with hydroxylamine, in which carboxylic acid and ketone functionalities would form hydroxamic acid and oximes, respectively. The significant broadening of a peak toward higher energy (up to 403 eV) in the N 1s core-level spectrum represented N−O bonds of oxime and hydroxamic acid and suggested the success of the functionalization. More importantly, the functionalization was accompanied by changes in its luminescence properties. The aqueous solution of NH_2OH-functionalized graphene QDs showed a blue-shift phenomenon. An excitation wavelength of 310 nm resulted in an emission maximum of 425 nm, as shown in Figure 5B.

Subsequent treatment with hydrazine hydrate was performed to reduce the highly oxidized graphene QDs. Hydrazine-reduced graphene oxide has been previously reported to contain N−N moieties of pyrazole structure whereby one of the N atoms is pyridinic-like, while the other is quaternary-like.[31] In fact, the presence of pyrazole was obvious in the N 1s core-level spectrum, as the peak at 401.2 eV, which corresponded to the presence of quaternary-like nitrogen atoms, was prominent. This particular peak for quaternary nitrogen was absent in the N 1s core-level spectrum of graphene QDs. Moreover, a N/C ratio of 0.28 registered by the hydrazine-reduced graphene QDs compared to 0.05 of graphene QDs signified the unintentional covalent functionalization with nitrogen moieties, mainly pyrazole, upon hydrazine treatment. Interestingly, the hydrazine-reduced graphene on graphene QDs resulted in a red-shift of the emission maximum to 520 nm when an excitation wavelength of 420 nm was applied, as shown in Figure 5C.

CONCLUSION

In conclusion, the present work has demonstrated the simultaneous oxidation and cage-opening of fullerene C_{60} to provide graphene quantum dots. The graphene QDs were synthesized by treating fullerene C_{60} with a mixture of concentrated sulfuric acid, sodium nitrate, and potassium permanganate. Detailed characterization including LDI-TOF MS, TEM, AFM, STM, XPS, DLS, FT-IR, and Raman spectroscopy analyses revealed the formation of aggregated small fragments consisting of carbon, oxygen, and hydrogen elements, which favored the production of graphene QDs. More importantly, the graphene QDs exhibited strong luminescence properties when excited at 340 nm. The highly oxygenated graphene QDs showcased their broad prospects for modifications through successful functionalization reactions. The luminescence properties varied according to the types of chemical treatments, whereby hydroxylamine-functionalized graphene QDs showed a blue-shift of the emission

maximum, while hydrazine-reduced graphene QDs showed a red-shift of the emission maximum. All in all, the simplicity of this method in producing graphene QDs shows potential for further development for integration into practical devices or applications including optoelectronics and biological labeling.

EXPERIMENTAL SECTION

Materials. The fullerene C_{60} (99.9%) was obtained from SES Research, TX, USA. Sulfuric acid (98%), potassium permanganate (99.5%), sodium nitrate (99.5%), hydrogen peroxide (30%), sodium hydroxide, hydrazine hydrate, and *N*,*N*-dimethylformamide (DMF) were obtained from Penta, Czech Republic. Hydroxylamine, 4-nitrobenzoyl chloride, and trifluoroacetic anhydride were obtained from Sigma-Aldrich, Czech Republic.

Procedures. *Synthesis of Graphene QDs.* The fullerene C_{60} was oxidized using Hummers method.[21] Fullerene C_{60} (2.5 g) and sodium nitrate (1.3 g) were stirred with sulfuric acid (98%, 57 mL). The mixture was then cooled to 0 °C. Potassium permanganate (7.5 g) was then added over a period of 2 h. During the next 4 h, the reaction mixture was allowed to reach room temperature before being heated to 35 °C for 30 min. The reaction mixture was then poured into a flask containing deionized water (125 mL) and heated to 70 °C for 15 min. The mixture was then poured into deionized water (0.3 L). The unreacted potassium permanganate and manganese dioxide were removed by the addition of 3% hydrogen peroxide. The reaction mixture was then neutralized using 1 M NaOH at pH = 8. The obtained graphene QD solution was purified by dialysis.

Reaction with Hydrazine Hydrate. Dialyzed graphene QDs (5 mL) were diluted with water (10 mL), and hydrazine hydrate (1 mL) was added. The reaction mixture was slightly alkalized with potassium hydroxide and heated under reflux for 24 h. Subsequently, the reaction mixture was concentrated under vacuum in order to remove unreacted hydrazine and to increase the concentration of graphene QDs. For the XPS analysis, 0.1 mL of the modified graphene QD solution was drop-casted onto a gold-coated silicon wafer and dried under vacuum for 5 h.

Reaction with Hydroxylamine. Dialyzed graphene QDs (5 mL) were diluted with water (10 mL), and hydroxylamine (1 mL) was added. The reaction mixture was heated under reflux for 24 h. Subsequently, the reaction mixture was concentrated under vacuum to remove unreacted hydroxylamine and to increase the concentration of graphene QDs. For the XPS analysis, 0.1 mL of modified graphene QD solution was drop-casted onto a gold-coated silicon wafer and dried under vacuum for 5 h.

Reaction with 4-Nitrobenzoyl Chloride. A dialyzed graphene QD solution (0.2 mL) was drop-casted onto a gold-coated silicon wafer and dried under vacuum. The wafer with graphene QDs was placed in 10 wt % of 4-nitrobenzoyl chloride in tetrahydrofuran (5 mL) for 24 h. Subsequently the wafer was removed from the solution, and unreacted 4-nitrobenzoyl chloride was washed off with dry THF and methanol and dried under vacuum at 50 °C for 24 h. The modified graphene QDs on the Au/Si wafer were directly used for XPS measurement.

Reaction with Trifluoroacetic Anhydride. A dialyzed graphene QD solution (0.2 mL) was drop-casted onto a gold-coated silicon wafer and dried under vacuum. The wafer with graphene QDs was placed on a holder over trifluoroacetic anhydride, and the flask was evacuated to 1 mbar. After 24 h, the wafer was removed from the trifluoroacetic anhydride atmosphere and dried under vacuum at 50 °C for 48 h. The modified graphene QDs on the Au/Si wafer were directly used for XPS measurement.

Equipment. An inVia Raman microscope (Renishaw, England) with a CCD detector was used for Raman and luminescence spectroscopy in backscattering geometry. A Nd:YAG laser (532 nm, 50 mW) with 50× magnification objective and He−Cd laser (325 nm, 22 mW) with 20× NUV objective were used for measurements. Instrument calibration was performed with a silicon reference which gave a peak centered at 520 cm^{-1} and a resolution of less than 1 cm^{-1}. In order to avoid radiation damage, the laser power output used for this measurement was kept in a range of 20 nW to 5 mW. Prior to measurements, the dialyzed sample was ultrasonicated for 5 min, and then the suspension was deposited on a small piece of silicon wafer and dried.

Fluorescence measurement was performed on a Cary Eclipse fluorescence spectrometer (Varian, USA). The measurement was performed in quartz glass cuvettes using 1 mL of the graphene QD suspension.

For the measurement of atomic force microscopy images, the dialyzed sample was ultrasonicated for 5 min and the suspension of graphene QDs was drop-casted onto a freshly cleaved mica substrate. These measurements were carried out on an Ntegra Spectra from NT-MDT. The surface scans were performed in tapping (semicontact) mode. Cantilevers with a strain constant of 1.5 $kN \cdot m^{-1}$ equipped with a standard silicon tip with curvature radius less than 10 nm were used for all measurements. The measurement was performed under ambient conditions with a scan rate of 1 Hz and scan line of 512.

For the measurement of scanning tunneling microscopy images, the dialyzed sample was ultrasonicated for 5 min and the suspension of graphene QDs was drop-casted onto freshly cleaved highly oriented pyrolytic graphite. These measurements were carried out on an Ntegra Spectra from NT-MDT. The surface scans were performed in a constant current mode using a Pt−Ir tip.

High-resolution X-ray photoelectron spectroscopy was performed on an ESCAProbeP (Omicron Nanotechnology Ltd., Germany) spectrometer equipped with a monochromatic aluminum X-ray radiation source (1486.7 eV). Wide-scan surveys with subsequent high-resolution scans of C 1s and O 1s core levels were performed. The relative sensitivity factors were used in the evaluation of the carbon-to-oxygen (C/O) ratios from the survey spectra. The dialyzed sample was ultrasonicated for 5 min, and the suspension of graphene QDs was drop-casted (0.1 mL) onto a layer of gold (200 nm) freshly evaporated on a silicon wafer.

The morphology and structure of the cage-opened fullerenes were studied by using HR-TEM JEOL JEM-3010 operated at 300 kV (LaB6 cathode and point-to-point resolution 0.19 nm). For investigation of graphene, the suspension with water (1 mg/mL) was ultrasonicated for 15 min (75 W) before use. As specimen support for TEM investigation, a microscopic copper grid covered by a thin transparent carbon film was used. The samples were studied in both bright field and electron diffraction (SEAD) modes.

Samples for laser desorption/ionization with time-of-flight detector mass spectrometry were prepared similarly to the method described by Kuckova *et al.*[32] Dialyzed graphene QDs were ultrasonicated for 5 min, and 1 μL was directly dropped on the steel sample plate and air-dried. The mass spectra were acquired in positive reflector (for masses in the range 0−2000 Da) with a mass accuracy of 0.4 Da on the Bruker-Daltonics Biflex IV mass spectrometer fitted with a standard nitrogen laser (337 nm, 120 μJ). The spectra were analyzed using the XMASS (Bruker) and mMass software.[33] Each mass spectrum was the result of at least 100 laser pulses. The spectra were calibrated by Pepmix (Bruker Daltonics, Germany).

Fourier transform infrared spectroscopy measurements were performed on a Nicolet 6700 FTIR spectrometer (Thermo Scientific, USA). A Diamond ATR crystal and DTGS detector were used for all measurements, which were carried out in the range 4000−400 cm^{-1} at a resolution of 2 cm^{-1}. A 0.1 mL amount of a dialyzed graphene QD suspension was drop-casted onto a silicon wafer and dried at room temperature. The measurement was performed directly on the material placed on the silicon wafer.

The dynamic light scattering was performed using a Zetasizer Nano ZS (Malvern, England). The measurement was performed at room temperature using disposable plastic cuvettes.

Conflict of Interest: The authors declare no competing financial interest.

Supporting Information Available: LDI-TOF MS analyses; particle size distribution analyses by DLS; HRTEM images; Raman and XPS spectra of fullerene C_{60}; luminescence properties from another batch of graphene QDs; XPS survey and high-resolution spectra of TFA-, NBC-, and NH_2OH-functionalized graphene QDs as well as hydrazine-reduced graphene QDs. This material is available free of charge *via* the Internet at http://pubs.acs.org.

Acknowledgment. M.P. acknowledges a Tier 2 grant (MOE2013-T2-1-056; ARC 35/13) from the Ministry of Education, Singapore. Z.S, P.Š., O.J., and K.K. were supported by Czech Science Foundation (Project GACR No. 15-09001S) and by specific university research (MSMT No. 20/2015).

REFERENCES AND NOTES

1. Kosynkin, D. V.; Higginbotham, A. L.; Sinitskii, A.; Lomeda, J. R.; Dimiev, A.; Price, B. K.; Tour, J. M. Longitudinal Unzipping of Carbon Nanotubes to Form Graphene Nanoribbons. *Nature* **2009**, *458*, 872–876.
2. Luo, J.; Cote, L. J.; Tung, V. C.; Tan, A. T. L.; Goins, P. E.; Wu, J.; Huang, J. Graphene Oxide Nanocolloids. *J. Am. Chem. Soc.* **2010**, *132*, 17667–17669.
3. Li, L.-s.; Yan, X. Colloidal Graphene Quantum Dots. *J. Phys. Chem. Lett.* **2010**, *1*, 2572–2576.
4. Bacon, M.; Bradley, S. J.; Nann, T. Graphene Quantum Dots. *Part. Part. Syst. Charact.* **2014**, *31*, 415–428.
5. Ponomarenko, L. A.; Schedin, F.; Katsnelson, M. I.; Yang, R.; Hill, E. W.; Novoselov, K. S.; Geim, A. K. Chaotic Dirac Billiard in Graphene Quantum Dots. *Science* **2008**, *320*, 356–358.
6. Shen, J. H.; Zhu, Y. H.; Yang, X. L.; Li, C. Z. Graphene Quantum Dots: Emergent Nanolights for Bioimaging, Sensors, Catalysis and Photovoltaic Devices. *Chem. Commun.* **2012**, *48*, 3686–3699.
7. Zhu, S. J.; Tang, S. J.; Zhang, J. H.; Yang, B. Control the Size and Surface Chemistry of Graphene for the Rising Fluorescent Materials. *Chem. Commun.* **2012**, *48*, 4527–4539.
8. Sun, H.; Wu, L.; Wei, W.; Qu, X. Recent Advances in Graphene Quantum Dots for Sensing. *Mater. Today* **2013**, *16*, 433–442.
9. Pan, D. Y.; Zhang, J. C.; Li, Z.; Wu, M. H. Hydrothermal Route for Cutting Graphene Sheets into Blue-Luminescent Graphene Quantum Dots. *Adv. Mater.* **2010**, *22*, 734–738.
10. Zhu, S. J.; Zhang, J. H.; Liu, X.; Li, B.; Wang, X. F.; Tang, S. J.; Meng, Q. N.; Li, Y. F.; Shi, C.; Hu, R.; *et al.* Graphene Quantum Dots with Controllable Surface Oxidation, Tunable Fluorescence and Up-Conversion Emission. *RSC Adv.* **2012**, *2*, 2717–2720.
11. Zhu, S. J.; Zhang, J. H.; Qiao, C. Y.; Tang, S. J.; Li, Y. F.; Yuan, W. J.; Li, B.; Tian, L.; Liu, F.; Hu, R.; *et al.* Strongly Green-Photoluminescent Graphene Quantum Dots for Bioimaging Applications. *Chem. Commun.* **2011**, *47*, 6858–6860.
12. Ye, R.; Xiang, C.; Lin, J.; Peng, Z.; Huang, K.; Yan, Z.; Cook, N. P.; Samuel, E. L. G.; Hwang, C.-C.; Ruan, G., *et al.* Coal as an Abundant Source of Graphene Quantum Dots. *Nat. Commun.* **2013**, *4*, 2943.
13. Dong, Y.; Lin, J.; Chen, Y.; Fu, F.; Chi, Y.; Chen, G. Graphene Quantum Dots, Graphene Oxide, Carbon Quantum Dots and Graphite Nanocrystals in Coals. *Nanoscale* **2014**, *6*, 7410–7415.
14. Shang, N. G.; Papakonstantinou, P.; Sharma, S.; Lubarsky, G.; Li, M. X.; McNeill, D. W.; Quinn, A. J.; Zhou, W. Z.; Blackley, R. Controllable Selective Exfoliation of High-Quality Graphene Nanosheets and Nanodots by Ionic Liquid Assisted Grinding. *Chem. Commun.* **2012**, *48*, 1877–1879.
15. Li, Y.; Hu, Y.; Zhao, Y.; Shi, G. Q.; Deng, L. E.; Hou, Y. B.; Qu, L. T. An Electrochemical Avenue to Green-Luminescent Graphene Quantum Dots as Potential Electron-Acceptors for Photovoltaics. *Adv. Mater.* **2011**, *23*, 776–780.
16. Yan, X.; Cui, X.; Li, L. S. Synthesis of Large, Stable Colloidal Graphene Quantum Dots with Tunable Size. *J. Am. Chem. Soc.* **2010**, *132*, 5944–5945.
17. Liu, R. L.; Wu, D. Q.; Feng, X. L.; Mullen, K. Bottom-Up Fabrication of Photoluminescent Graphene Quantum Dots with Uniform Morphology. *J. Am. Chem. Soc.* **2011**, *133*, 15221–15223.
18. Lu, J.; Yeo, P. S. E.; Gan, C. K.; Wu, P.; Loh, K. P. Transforming C60 Molecules into Graphene Quantum Dots. *Nat. Nanotechnol.* **2011**, *6*, 247–252.
19. Kroto, H. W.; Heath, J. R.; Obrien, S. C.; Curl, R. F.; Smalley, R. E. C60: Buckminsterfullerene. *Nature* **1985**, *318*, 162–163.
20. Hirsch, A.; Brettreich, M.; Wudl, F. *Fullerenes: Chemistry and Reactions*; Wiley, 2006.
21. Hummers, W. S.; Offeman, R. E. Preparation of Graphitic Oxide. *J. Am. Chem. Soc.* **1958**, *80*, 1339–1339.
22. Chua, C. K.; Sofer, Z.; Pumera, M. Graphene Sheet Orientation of Parent Material Exhibits Dramatic Influence on Graphene Properties. *Chem.—Asian J.* **2012**, *7*, 2367–2372.
23. Mcelvany, S. W.; Ross, M. M.; Callahan, J. H. Characterization of Fullerenes by Mass-Spectrometry. *Acc. Chem. Res.* **1992**, *25*, 162–168.
24. Jankovsky, O.; Hrdlickova Kuckova, S.; Pumera, M.; Simek, P.; Sedmidubsky, D.; Sofer, Z. Carbon Fragments are Ripped Off from Graphite Oxide Sheets during Their Thermal Reduction. *New J. Chem.* **2014**, *38*, 5700–5705.
25. Schniepp, H. C.; Li, J.-L.; McAllister, M. J.; Sai, H.; Herrera-Alonso, M.; Adamson, D. H.; Prud'homme, R. K.; Car, R.; Saville, D. A.; Aksay, I. A. Functionalized Single Graphene Sheets Derived from Splitting Graphite Oxide. *J. Phys. Chem. B* **2006**, *110*, 8535–8539.
26. Ravindran, T. R.; Jackson, B. R.; Badding, J. V.; Raman, U. V. Spectroscopy of Single-Walled Carbon Nanotubes. *Chem. Mater.* **2001**, *13*, 4187–4191.
27. Gruen, D. M. Nanocrystalline Diamond Films. *Annu. Rev. Mater. Sci.* **1999**, *29*, 211–259.
28. Ferrari, A. C. Raman Spectroscopy of Graphene and Graphite: Disorder, Electron-Phonon Coupling, Doping and Nonadiabatic Effects. *Solid State Commun.* **2007**, *143*, 47–57.
29. Chua, C. K.; Sofer, Z.; Pumera, M. Graphite Oxides: Effects of Permanganate and Chlorate Oxidants on the Oxygen Composition. *Chem.—Eur. J.* **2012**, *18*, 13453–13459.
30. Chua, C. K.; Pumera, M. Selective Removal of Hydroxyl Groups from Graphene Oxide. *Chem.—Eur. J.* **2013**, *19*, 2005–2011.
31. Park, S.; Hu, Y.; Hwang, J. O.; Lee, E.-S.; Casabianca, L. B.; Cai, W.; Potts, J. R.; Ha, H.-W.; Chen, S.; Oh, J.; *et al.* Chemical Structures of Hydrazine-Treated Graphene Oxide and Generation of Aromatic Nitrogen Doping. *Nat. Commun.* **2012**, *3*, 638.
32. Kuckova, S.; Hynek, R.; Nemec, I.; Kodicek, M.; Jehlicka, J. Critical Comparison of Spectrometric Analyses of Non-Mineral Blue Dyes and Pigments Used in Artworks. *Surf. Interface Anal.* **2012**, *44*, 963–967.
33. Strohalm, M.; Hassman, M.; Kosata, B.; Kodicek, M. Mmass Data Miner: An Open Source Alternative for Mass Spectrometric Data Analysis. *Rapid Commun. Mass Spectrom.* **2008**, *22*, 905–908.